14

Screen Printed Electrodes with Improved Mass Transfer

Jan Krejci, Romana Sejnohova,
Vitezslav Hanak and Hana Vranova
BVT Technologies, a.s., Hudcova 533/78c, 612 00 Brno,
Czech Republic

1. Introduction

Electrochemical sensors in contrast to many other analytical methods enable possibility of their production at low price and their miniaturization. The first feature leads to their possibility massive application in industry, home products and as input devices of computers. The possibility of electrochemical sensor preparation in micro-scale enables creation of arrays and fields of sensors on chips of size of some square of mm. Despite of these excellent properties the electrochemical sensors are not widely spread in practice. Despite of their massive research and development, their penetration into the practise is slow. They suffer by some weaknesses namely in reproducibility. Only very skilled experts obtain reliable and reproducible results by their use. The survey of patent literature, scientific and economical literature prove that the advantages of electrochemical sensor are without discussion however the journey to use their advantages in practise is more difficult and complicated than it can be supposed after first positive experiments. This can by approved by examples. The development of glucose chips for diabetic patients took more 20 years. In early 90ties the lost from their production was in millions of GBP per year. The development of colourometric diagnostic strips takes significantly less time than 10 years dry chemistry. They were used as diabetic strips till middle of 90ties. The advantage of electrochemical sensors wins but it was very difficult and expensive development. In end of 70ties many companies stated (Krejčí, 1988) that implantable sensor of glucose will be in market in months. After 30 years does not exist reliable implantable sensor of glucose on market. Ten years ago it was stated that electrochemical DNA sensor array will be important analytical tool but only optical arrays are routinely used now. Generally after first results which can be obtained in very easy manner in electrochemical sensors the development to final device is at least two times longer than optical methods or other methods where the first experiments are quite complicated e.g. Surface Plasmon Resonance (SPR) (Frost & Sullivan, 1994; Sethi et al., 1989, 1990).There are many reasons which are behind low robustness of electrochemical sensors. One of them is mass transport between bulk of sample and active sensor area. The background of this phenomenon is in fig. 1.

On the surface of an electrochemical sensor there are three layers defining its response. The first layer of specially adsorbed ions and molecules is called the compact Helmholz layer (sometimes Stern layer). This is defined by centres of atoms "sitting" on the electrode

a) (b)

Fig. 1. Difference between electrochemical (a) and optical (b) measurement.

surface. The locus of electrical centres of ions adsorbed in the Helmholz layer (more precisely centres of symmetry of ion electrical field) is called the inner Helmholz plane. The outer Helmholz layer is formed by the space charge region which is created by interaction between electrode and charged ions in solutions. The outer Helmholz plane is the locus of centres of the nearest solvated ions with respect of to the electrode surface (Bard & Faulkner, 1980). The third layer is created by Nernst layer where the concentration differs from the bulk concentration due to the diffusion of electro active compounds to the electrode surface. The response of the sensor will depend on the structure of each of these layers and on the chemical reactions which run in each of these layers. There are also fluctuations of properties of each of this layer. It is obvious that these fluctuations will be averaged on the electrode surface but not in the distance x. The electrochemical biosensor is prepared from electrochemical sensor by immobilization of bioactive compound (Macholán, 1991; Turner et al., 1987). The immobilized layer lies in the outer Helmholz layer and in the Nernst layer. It assures not only the run of reaction which is responsible for sensor selectivity but it influences the structure of inner Helmholz layer. The process of immobilization significantly changes the specific adsorption on the active electrode. The influence of bioactive layer on the structure of outer Helmholz layer and Nernst layer is dramatic. The bioactive membrane changes the space distribution of the charge, solvation processes, pH equilibration in outer Helmholz layer. The bioactive layer also changes the concentration distribution in Nernst layer. The interactions are mutual. The presence of electrode and reactions on its surface influences the bioactive membrane. The local changes of pH can move the reaction out of pH optimum. Local changes of ionic strength can influence the reaction in bioactive membrane (Kotyk et al., 1977). The situation with optical sensor is quite different. The beam of light goes trough the analyzed solution and interacts with molecules. It interacts directly with each molecule and there is no subsequent interaction in layer as in the case of electrochemical sensors. Fluctuations in optical measurement also occur however these will be averaged not only on the optical detector surface but also along the distance x along, the path of beam. It assures better robustness of optical measurement. This demonstrates the important role played by mass transport in electrochemical measurements and in electrochemical biosensors (Dvořák & Koryta, 1983; Rieger, 1993; Riley, et al. 1987). The role of mass transport can be shown experimentally. It is possible to measure the surface of screen printed electrodes by SEM and confocal microscopy and compare the result with

electrochemical measurement. This procedure is in detail described in (Schröper et al., 2008). The importance of this measurement consists not only in the fact of obtaining the active area of the sensor but experiments these can be considered as model of typical amperometric measurement. The result is in fig. 2 and fig. 3.

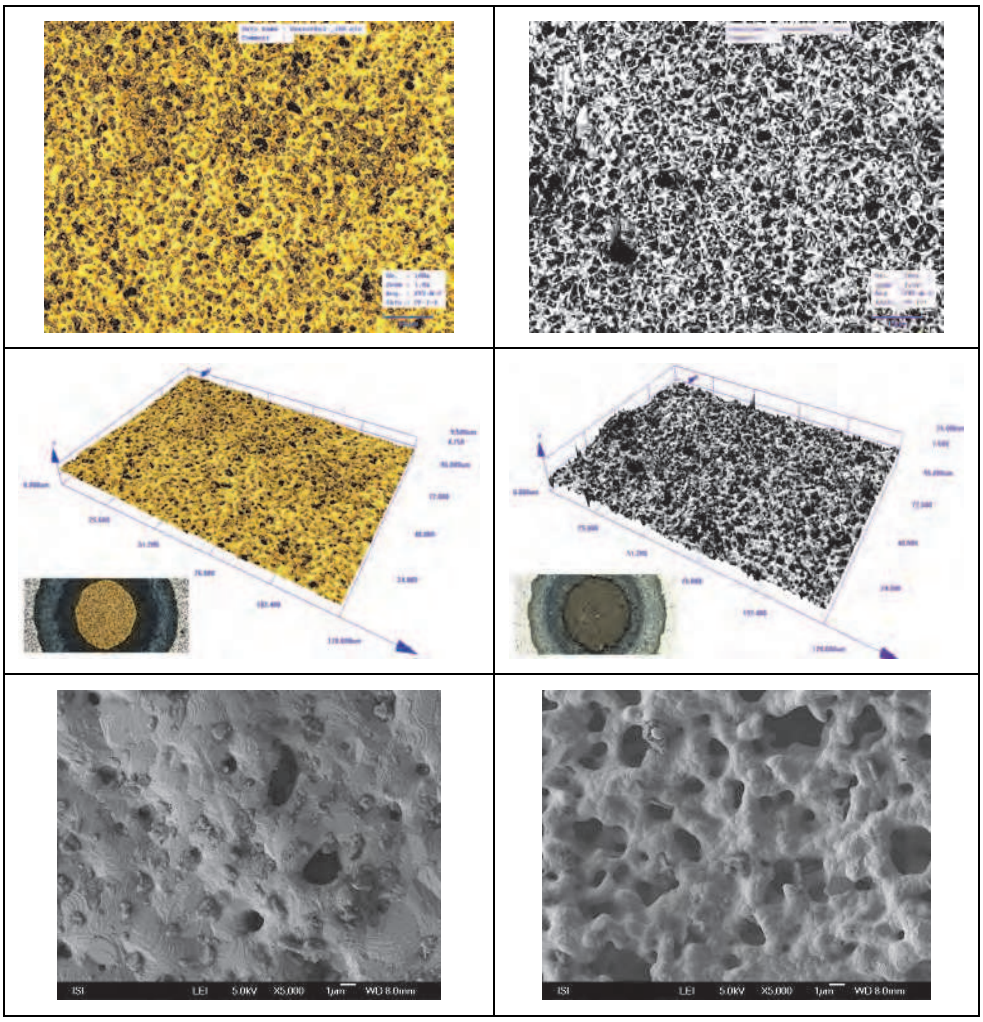

Fig. 2. The surface structure of AC1.W1.RS (left panel) and AC1.W2.RS (right panel) recorded by optical (upper and middle part) and scanning electron microscopy (bottom part).

Fig. 2 shows the anaysis of gold and platinum active surface of electrodes by optical microscopy and scanning electron microscopy. The comparison with electrochemical measurement is in fig. 3. Independent methods show the active surface significantly bigger as electrochemical measurement.

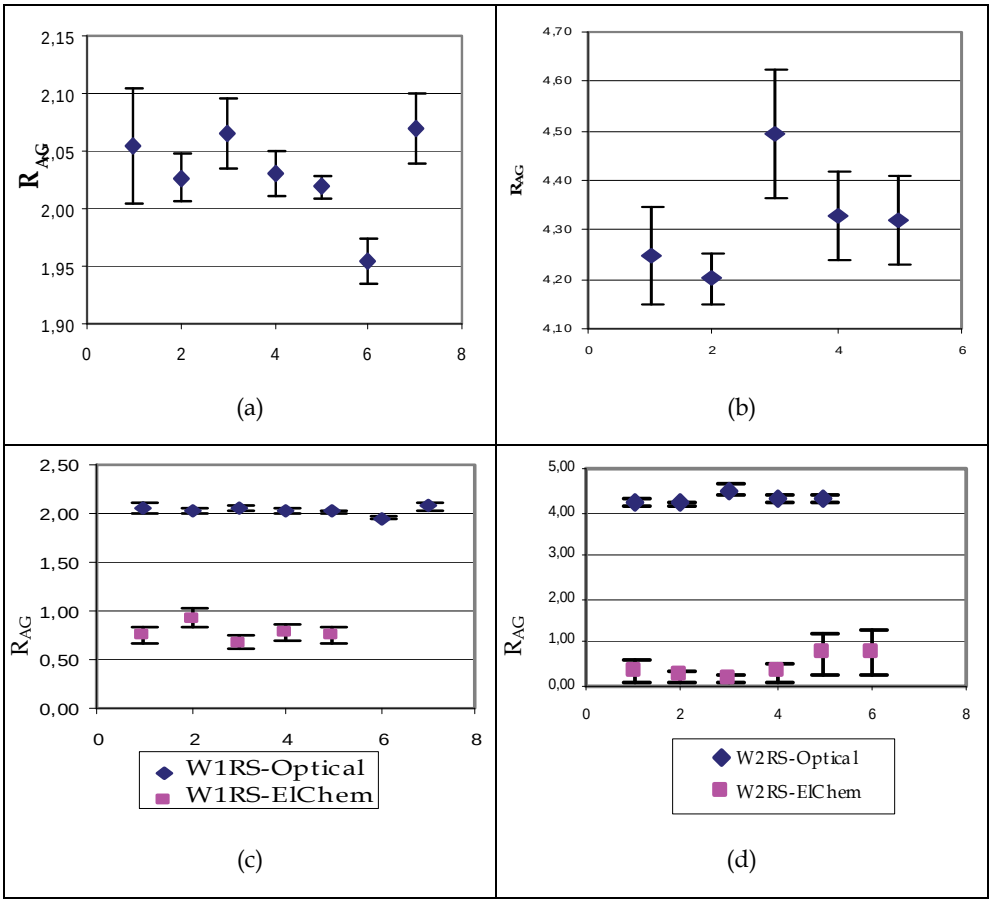

Fig. 3. The results of confocal microscope relation of active area to geometrical area (R_{AG}) measurement, a) (R_{AG}) for the sensor AC1.W1.RS (Au) b) (R_{AG}) for the sensor AC1.W2.RS (PT). Comparison with electrochemical measurement c) Sensor AC1.W1.RS (Au) d) Sensor AC1.W2.RS (Pt).

The surface properties of Au and Pt working electrodes prepared by screen printing (BVT Technologies, a.s.) were studied on statistical data sets. The mean ratio of active to geometrical surface (R_{AG}) obtained by optical measurement is in Tab. 1.

Type of sensor	Working electrode	R_{AG}	Number of measurements
AC1.W1.RS	Au	2.03 ± 0.04	(n = 7)
AC1.W2.RS	Pt	4.35 ± 0.08	(n = 5)

Table 1. Optical measurement

(R_{AG}) obtained by electrochemical measurement of the same sensors. Results for AC1.W1.RS and AC1.W2.RS are as follows (Tab. 2).

Type of sensor	Working electrode	R_{AG}	Number of measurements
AC1.W1.RS	Au	0.61 ± 0.06	(n = 5)
AC1.W2.RS	Pt	0.34 ± 0.20	(n = 6)

Table 2. Electrochemical measurement

Electrochemical results are approximately an order of magnitude lower than optical measurement data (3x, 12x).
The simplest explanation for this difference can be explained by insufficient mass transport and its poor reproducibility. The electrochemical reaction runs only on the upper edges of the complicated electrode surface. This reaction shields the lower layers of the electrode where no reaction takes place (see fig. 4). It is obvious that mass transport under such conditions will be very sensitive to experimental arrangement namely stirring of the solution. This also explains the difference between electrochemical determinations of active surface measurement in the literature where results can differ in range by one order. This shielding explains the low efficiency of nanostructures on the electrode surface (Fig. 4) which was indirectly confirmed by experiments in (Maly et al., 2005). These results are valid not only for special measurement as mentioned above but more generally for all measurements based on the electrochemical principle.

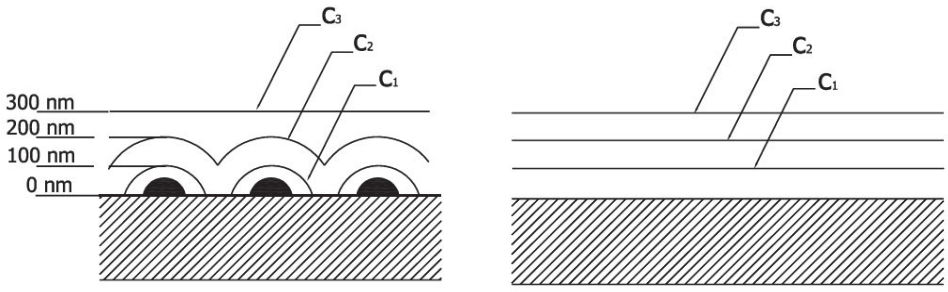

(a) (b)

Fig. 4. Nanostructured (a) and planar (b) electrode of electrochemical sensor.

2. Properties by controlled mass transport

In the next section the improvement of screen printed electrochemical sensors and biosensor will be demonstrated and wall jet cell by three techniques

- Microfluidic arrangement which uses a thin layer cell
- Rotated disc microelectrode
- Thermodiffusion

The improvement is based on controled and amplified mass transport from bulk of solution to the active surface of electrode.

2.1 Microfluidic arrangement

The experimental arrangement of the microflow system (MFS) is illustrated in figure 5.

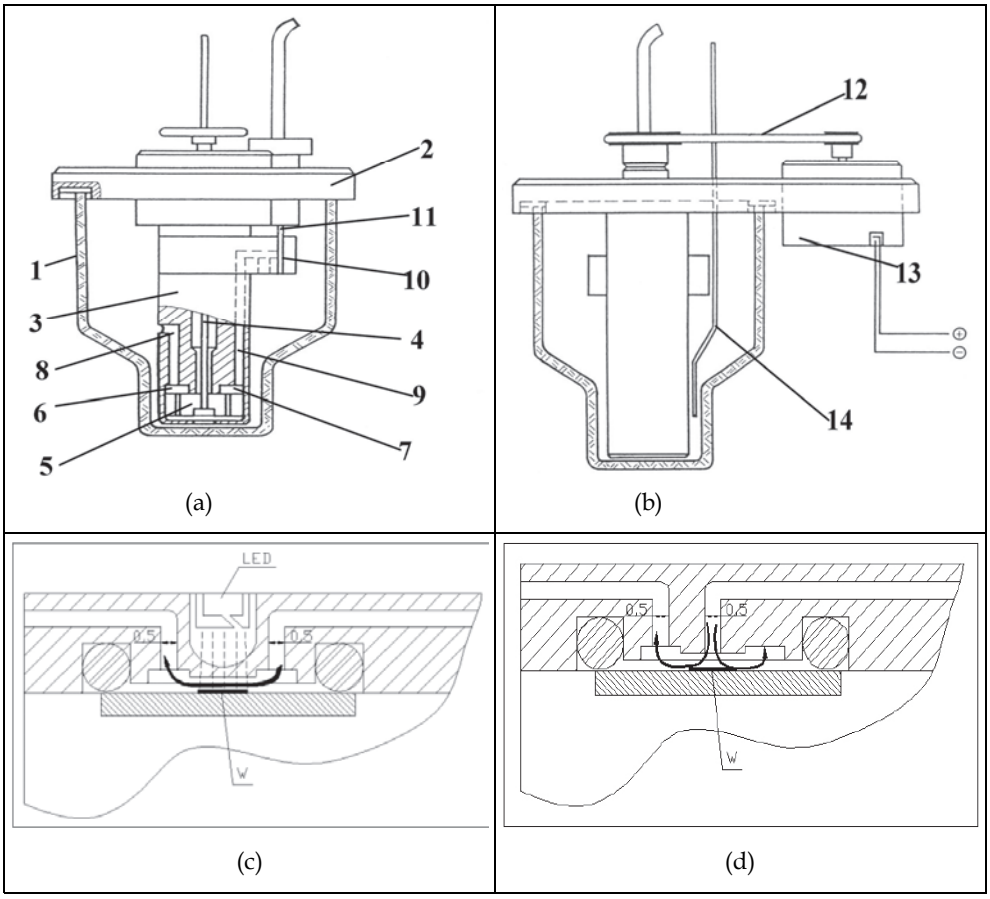

Fig. 5. a,b) Experimental arrangement of the Microflow system (Patent CZ 287676); 1) electrochemical vessel, 2) modified lid, 3) body of microflow insert, 4) driving shaft, 5) pump rotor, 6) sample mixing chamber, 7) sample pumping chamber, 8) mixing channel outlet, 9) capillary, 10) microflow chamber, 11) thick film sensor, 12) mixing channel inlet, 13) driving belt, 14) motor, 15) inert gas input. c) Flow cell arranged in thin layer format. d) Flow cell arranged in wall-jet format (Krejci et al., 2008).

A conventional electrochemical vessel (Rieger, 1993) (1) in figure 5 (TC1) (BVT Technologies, a.s., Czech Republic) is covered by a modified lid (2) carrying the body of the microflow insert (3). The driving shaft (4) located in the centre of the microflow insert is connected to the pump rotor (5) immersed in the electrolyte/sample fluid. The electrolyte/sample fluid comes to the pump rotor (5) via mixing channel inlet (12). The two chambers located above the rotor fulfil two different functions. The first of the chambers (6) is connected via mixing channel outlet (8) to the bulk of electrolyte/sample solution inside the electrochemical vessel. The portion of the liquid being pumped through this passageway provides for sufficient stirring of the solution inside the electrolyte vessel. The second chamber (7) helps to guide the fluid coming from the rotor into the capillary (9) and into the electrode cell (10).

The function of the narrow capillary is to stabilize the flow of the liquid before it enters into the electrode cells. The overall design of the insert is such that only 1 – 5% of the liquid is flowing through the chamber (7) and capillary (9), while bout 95 – 99% of it is pumped through the chamber (6): and channel (8), ensuring intensive stirring of the solution. The electrode cell (10) contains the integrated three-electrode amperometric sensor (11) (AC1.W2.R1, BVT Technologies, a.s., Czech Republic; Fig. 6b). Following its passage past the sensor, the liquid is returned from the electrode cell directly into the bulk of the electrolyte/sample solution inside the vessel. The driving shaft (4) is connected by means of an elastic belt (13) to the external motor (14). The entire electrochemical vessel with the microflow insert immersed in the electrolyte/sample solution is placed in a thermostat bath and the temperature is kept constant at 25 ± 0.1 °C. The tube (15) can be used for inert gas introduction for work under inert atmosphere. A few other openings in the lid (2) are provided for sample additions, insertion of a thermometer and for other accessories. The arrangement is mainly destined for batch injection analysis. The principle was integrated into the device MFS (BVT Technologies, a.s.) (Fig. 6a) (Krejci et al., 2008).

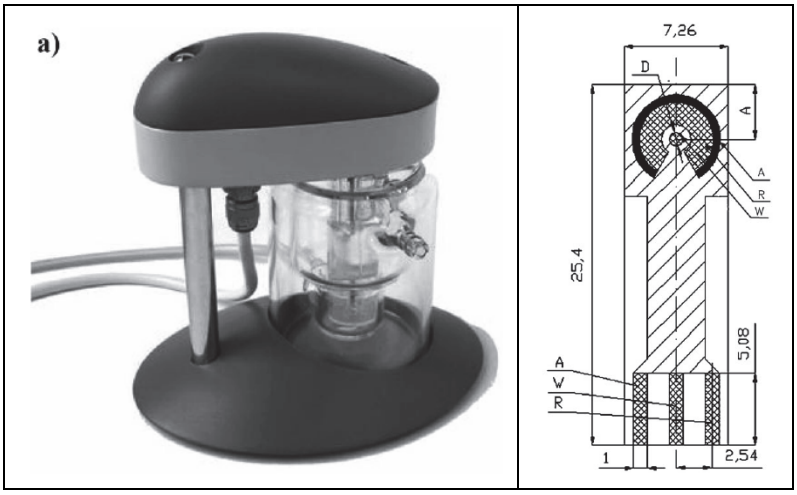

Fig. 6. a) Photo of the microflow system (MFS) device (BVT Technologies, a.s., Czech Republic). b) Integrated three-electrode amperometric sensor (Patent CZ 291411) (A: auxiliary electrode, R: reference electrode, W: working electrode) (Krejci et al., 2008).

The device can be equipped with two types of electrode cells (fig. 5, 10). The wall jet cell and thin layer cell (fig. 5 c, d). In case of wall jet cell the stream of analyte flows from small orifice of diameter a perpendicularly to the active surface of electrode. The current of electrode in wall jet arrangement where the diameter of electrode active area is bigger than jet opening is described by equation (1) (Painton & Mottola, 1983). The theory of wall-jet hydrodynamic arrangement was originally derived by Matsuda (Matsuda, 1967; Yamada & Matsuda, 1973). The more detailed description of jet flow is in excellent monography of Polyanin (Polyanin et al., 2002).

$$I = 1{,}15\ n\ F\ R^{3/4}\ a\ D^{2/3}\ \upsilon^{-5/12}\ U^{3/4}\ c_0 \tag{1}$$

where
n-Number electrons in reaction; F-Faraday constant [96 485 C.mol^{-1}]; R-Radius of electrode [m]; a-Diameter of jet [m]; D-Diffusion coefficient [m^2.s^{-1}]; υ-Kinematic viscosity [m^2.s^{-1}]; U-Velocity in the jet [m.s^{-1}]; c_0-Concentration [mol.l^{-1}]; I-Current [A]
The important characterization of the cell is its conversion efficiency η. This quantity describes the relation of actual current with respect of current produced by all electroactive (active in case of biosensor) compounds entering the cell. Using data from Polyanin (Polyanin et al., 2002) it can be evaluated as

$$\eta = \frac{4 \times 1.15}{\pi^{3/4}} R^{3/4} D^{2/3} \upsilon^{-5/12} Q^{-1/4} a^{-1/2} \tag{2}$$

where
Q-volume flow of sample trough cell [m^3.s^{-1}]
The thin layer arrangement is characterized by electrode active surface placed in channel with very small height. Important characterization of thin layer arrangement is that channel height h is significantly smaller than channel width b (h << b) (see fig. 5c). There are many different equations in literature which describes thin layer hydrodynamic arrangement. They can by summarized as equation (4a) where different authors found different value of constant k (Brunt & Bruins, 1979; Hanekamp & Nieuwkerk, 1980; Levich, 1947; Wranglén et al., 1962). If the flow around electrode is stable and laminar then Matsuda derived equation (4b) (Matsuda, 1967). More recent and excellent discussion namely concentrated on was made by (Squires, 2008). Comprehensive analysis is also in (Polyanin et al., 2002). If the length of electrode in the channel is higher than l (equation 3) then the sensor measures in coulometric mode with 100% conversion. All electrochemical compounds are reacted/converted at the electrode. In summary the current in case of thin layer cell is described by equation (4c).

$$l \geq \frac{3}{8} \frac{h}{b} \frac{Q}{D} \tag{3}$$

where
D-Diffusion coefficient [-]; b-width of the channel [m]; h-channel height [m]; l-length of electrode [m]

$$I = k\, n\, F\, D^{2/3}\, b\, l^{1/2}\, \upsilon^{-1/6}\, U^{1/2}\, c_0 \tag{4a}$$

$$I = 1,47\, n\, F\, D^{2/3}\, A\, b^{-2/3}\, U^{1/3}\, c_0 \tag{4b}$$

$$I = n\, F Q c_0 \tag{4c}$$

where
k-lies in the range 0.68 – 0.83; b-width of the channel and electrode covering the wall of the channel [m]; U-the linear velocity with laminar flow [m.s^{-1}]; A-electrode area [m^2]; Q-volume flow of electro-active material [m^3. s^{-1}]
The meaning of rest of symbols is same as in previous equations.
The conversion efficiency in above three cases is in equation (5)

$$\eta = k\, D^{2/3} \left(\frac{Qh}{lb} \right)^{-1/2} \upsilon^{-1/6} \quad \text{for (4a)} \tag{5a}$$

$$\eta = 1.47\, D^{2/3} \left(\frac{Q}{h} \right)^{-2/3} \quad \text{for (4b)} \tag{5b}$$

$$\eta = 1 \quad \text{for (4c)} \tag{5c}$$

2.2 Rotated disc microelectrode

A rotating disc electrode (RDE) is one exceptional example where the hydrodynamics (Navier stokes equations) and convective mass transport can be solved in analytical approximation. This means that relatively simple formulas exist that describe the electrode response with sufficient precision. (Some authors states that the hydrodynamics and convective diffusion at RDE can be analytically solved but this is not true.) The main principles of RDE are theoretically described in the literature (Bard & Faulkner, 1980; Riger 1993; Riley et al., 1987) for example. However the exact and comprehensive description of RDE physics can be found in Levich's works (Levich, 1942, 1944, 1944, 1947). The results are summarized in (Levich, 1962). The Levich derivation is based on results of Karman (Karman, 1921). These results are used not only in Levich's derivation but in many recent works. Comprehensive analysis of RDE principle is in literature (Sajdlová, 2010; King et al., 2005). An example of a RDE is shown in fig. 7. Classical RDE involve a platinum wire within glass tubing sealed in the plastic body of the RDE. The shape of the insulating mantle has an important role for the RDE function. It is obvious from the fact that Levich equation (6) describing RDE response is valid for disc of infinite radius in semi infinite homogenous media. This condition can not be fulfiled in real experimental conditions. However the thickness of hydrodynamic boundary layer (δ0) is significantly lower than electrode diameter. If the electrode is placed in distance from bottom of reaction vessel which is at least 1 order bigger than (δ0) then Levich equation will be very good approximation of RDE function. It means if the low angular speed is used the active surface of electrode is placed at least 10 mm above bottom of reaction vessel (see tab. 3). Corruption of this condition leads to hydrodynamic instability (Sajdlová, 2010). The electrical connection on the opposite end is made by the means of a brush contact. The noise of electrode significantly depends on the contact material and its construction. Will be had best experience with gold contact and precious metal brush. The RDE can be prepared also as disposable insert (fig. 7) where the active surface is made by screen-printing. The main advantage of RDE consists of possibility to control the mass transport by rotation speed. If the experiments are done at different velocities then the response can be extrapolated to infinite rotation speed where the mass transport is eliminated and the response is determined by electrode kinetic only or by immobilized enzyme kinetic if RDE is used as biosensor. It enables the optimization of immobilization procedure including precise measurement of membrane properties including enzyme biosensor membrane characterization. The RDE is characterized by two most important parameters: δ0 – thickness of the hydrodynamic boundary layer and thickness of Nernst diffusion layer (δ), where the maximum changes of concentration with respect of bulk concentration take place. Both parameters depend on angular velocity and they can be expressed, as is shown in equations (6) and (7) (Levich, 1962).

$$\delta_0 = 3.6\sqrt{\frac{\upsilon}{\omega}} \tag{6}$$

$$\delta = 0.5\sqrt[3]{\frac{D}{\upsilon}}\,\delta_0 \tag{7}$$

where
υ- kinematics viscosity; ω-angular velocity; D-diffusion coefficient of analyte
Due to power 1/3 the dependence on υ is small. The typical values of δ_0 and δ for H2O and glycerol are shown in table 3.

ω [s-1]	H2O		glycerol		Time resolution [s]
	δ_0 [μm]	δ [μm] (D = 10-10 m2.s-1)	δ_0 [μm]	δ [μm] (D = 10-10 m2.s-1)	
1	1000	50	33000	33	16
10	330	16.5	10000	10	2.2
100	100	5	3300	3.3	0.16
1000	33	1.6	1000	1	0.022

Table 3. Typical values for H2O and glycerol.

The knowledge of the diffusion boundary layer enables to estimate the time resolution of measurement as with RDE $\tau \doteq \frac{\delta^2}{D}$. The typical values are in table 3 too.
The output current of RDE is derived from the Levich equation.

$$I = 0.620\, n\, F\, A\, D^{2/3}\, \upsilon^{-1/6}\, \omega^{1/2}\, c_0 \tag{8}$$

where
n-Number of electron in the reaction,; F-Faraday constant [96 485 C.mol^{-1}]; A-Area of Electrode [m^2]; D-Diffusion coefficient [m^2.s^{-1}]; υ-Kinematic viscosity [m^2.s^{-1}]; ω-Angular velocity [s^{-1}]; c_0-Concentration [mol.l^{-1}]; I-Current [A]
The conversion efficiency of RDE is

$$\eta = 0{,}697\left(\frac{D}{\upsilon}\right)^{2/3} \tag{9}$$

The conversion efficiency does not depend on electrode rotation speed and electrode diameter. It values for small molecules in water is $\eta_{H2O} \sim 0.01$ and for glycerol $\eta_{glycerol} \sim 10^{-4}$.
Equations (1, 4 and 8) are confirmed in the literature (King et al., 2005; Masavat' et al., 2008; Painton & Mottola, 1983; Tóth et al., 2004). Nearly all publications use these equations with improper description of quantities, and improper coefficients. We have checked these equations in the original literature and confirmed their validity. The fact, that majority of publications which uses the equations (1, 4 and 8) for evaluation of electrode parameters or membrane parameters, uses wrong equations; introduce some doubts about their reliability and reliability of published data where these equations were used for calculation of

diffusion coefficient or other parameters. In analytical practice the use of wrong formulas does not play much important role because the measurement is calibrated and all equation (1, 4 and 8) has a general structure I = konst c_0. On the other hand it proves that the results are not comparable between different experimental arrangements without cross calibration. Implicitly the above low reliability of measurement is nothing else than insufficient definitions of mass transport. All equations (1, 4 and 8) are nothing else than solution of mass transport to the electrode under special conditions.

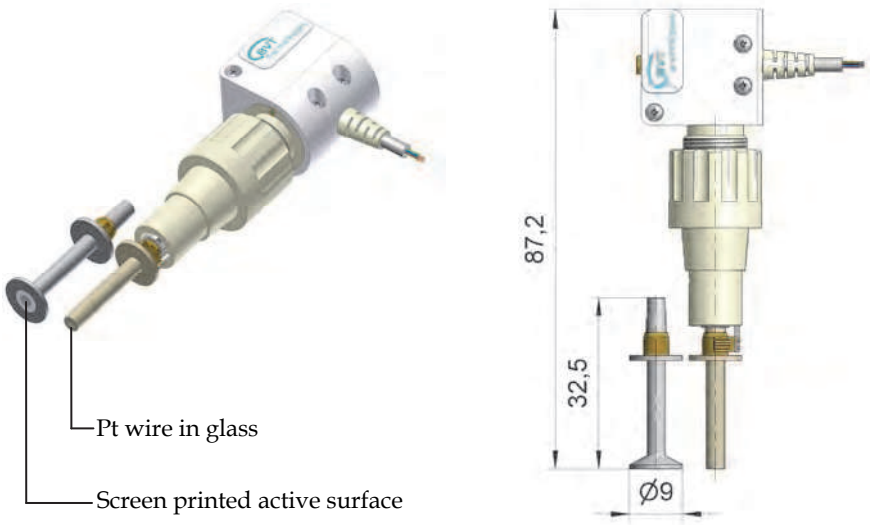

Fig. 7. a, b) Mini-rotated disc electrode

The principle of RDE can be enhanced to move complicated hydro-dynamical arrangement. It can be used for elimination of cross talk of array of electrodes (Dock et al., 2005; Sajdlová, 2010).

The comparison of conversion efficiencies for typical parameters used in measurement in experimental part are summarized in tab. 4.

The parameters are:

diameter of jet nozzle a = 0.5 mm; radius of electrode R = 1 mm; height of channel h = 0.3 mm; width of channel b = 1 mm; length of electrode l = 2 mm; diffusion coefficient $D = 10^{-9}$ m^2 s^{-1}; kinematics' viscosity of water $\upsilon = 10^{-6}$ m^2 s^{-1}; angular speed of RDE $\omega = 60$ s^{-1}

ηw (equation 2)	5 . 10-2
η5a (equation 5a)	3 . 10-2
η5b (equation 5b)	1 . 10-3
ηRDE (equation 9)	1 . 10-2
Hchannel (equation 3)	100 mm

Table 4. Comparison of different conversion efficiencies for typical parameters of cell listed in text.

2.3 Thermodiffusion

Electrochemical measurements are generally done under isothermal conditions. Thermal gradient can be also used to improve the mass transport. The application of a controlled temperature gradient between the working electrode surface and the solution, using electrochemical sensors prepared on ceramic materials with extremely high heat conductivity, enables that applied thermal gradient creates a the second driving force of mass transport. This application of the Soret phenomenon increases the mass transfer in the Nernst layer and enables more accurate control of the electrode response enhancement by a combination of diffusion and thermodiffusion. The key physical phenomenon is difference of thermal conductivity of ceramic and water solutions. The thermal conductivity of Al_2O_3 ceramic is about 35 $Wm^{-1}K^{-1}$. The thermal conductivity of water is 0.6 $Wm^{-1}K^{-1}$. If the active electrode is printed on the ceramic where on its opposite side just under working electrode is placed heating then the thermal gradient can be significantly higher than concentration gradient. The thermodiffusion coefficient is about 1-3 % of diffusion coefficient but at high temperature gradients the thermodiffusion mass flow can be comparable with mass flow driven by concentration gradient. It is important that thermodiffusion driving force can be adjusted independently on the concentration by temperature of sensor. Cotrell-Soret equation (10) has been derived in the literature (Krejčí, 2010).

$$I = n\,F\,A\,C_0\,\frac{D}{1+\theta(T_1)}\,s_T\,\alpha\,(T_1 - T_2) \tag{10}$$

where

$$\theta(T_1) = e^{\left(\frac{nF\left(E-E^0\right)}{RT_1}\right)}$$

$\theta(T_1)$ stresses the fact that due to high temperature conductivity of ceramic substrate of the sensor, the temperature T_1 of the electrode surface is known. The Cotrell-Soret equation has significant advantage with respect to Cotrell equation as it does not depend on the time. The derived the Cotrell-Soret equation describing the steady-state response with an applied temperature difference enables the measurement of electrode equilibrium potential at given temperature.

The termodiffusion can remove the accumulation of reduced/oxidised compounds at closed neighbourhood of electrode which is responsible for the hysteresis and complicated form of cyclic voltametry (CV) response. The example of use of thermodiffusion for sensor response improvement shows the ability of use of microelectronic technologies in electrochemical sensor production. The screen-printed active electrode together with screen-printed heaters and integrated thermometer Pt 1000 creates the electrochemical device which does not have classical analogy.

2.4 Experimental

The above discussion about mass transport will be demonstrated on four examples which demonstrate that screen-printed electrochemical sensor is very precise and sensitive device. These examples are amperometric measurement of H_2O_2, which is important for biosensors application where H_2O_2 is product of enzymatic reaction (oxydases); measurement of glucose oxidase by electrochemical sensor with immobilized enzyme; fast measurement of enzyme activity; cyclic voltammetry at temperature gradient.

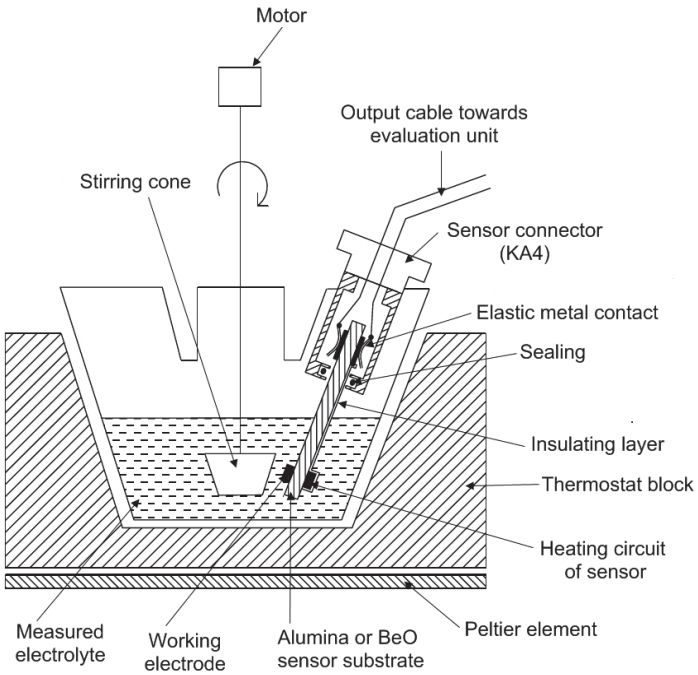

Fig. 8. Schematic of the Soret system (the gap between the cone and electrode surface is 1 mm)

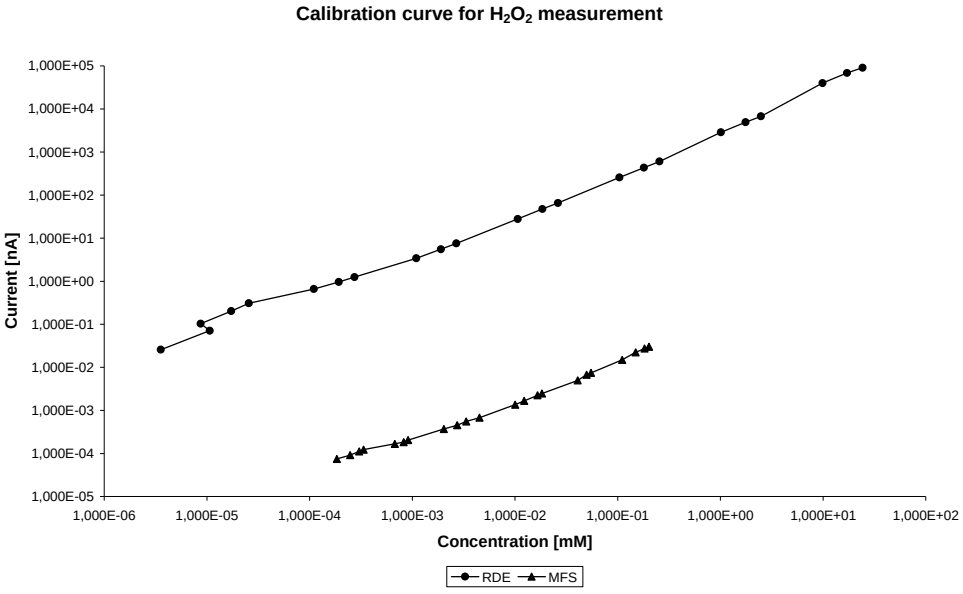

Fig. 9. Calibration curve for H_2O_2 measurement (Krejci et al., 2008).

2.4.1 Amperometric measurement of H_2O_2

The standard solution of hydrogen peroxide was prepared from a 3% stock solution (Lachema, Brno, Czech Republic). The electrochemical vessel filled with 5.00 ml of the working electrolyte (50 mM phosphate buffer, pH 7.0). The measurement was initiated by recording the background current in the absence of an analyte. After its stabilization, addition 50 μl aliquots of analytes (hydrogen peroxide) the changes in the current were recorded. Detection of hydrogen peroxide was carried out by amperometric measurement at the platinum working electrode of the AC1.W2.R1 sensor. The reaction chamber was wall-jet (see fig 5). Figure 9 shows the response to stepwise concentration changes of hydrogen peroxide spanning the range between 1.1 x 10^{-9} to 8 x 10^{-3} M. The extremely wide measurement range and very low limit detection is result of working electrode nanostructure (see fig. 2) and optimized mass transport in MFS device. The electrode is sintered from Pt grains of size 100 – 1000 nm, which assures extremely large active area as it is seen in fig. 2. Measurement was carried out with RDE under the same conditions. The angular velocity was $\omega = 60\ s^{-1}$. Experiments were done in 5 ml solution of phosphate buffer and 50 μl aliquots of different concentrations of H_2O_2 were added. The results are in the fig. 9 too. Under this condition the time the time resolution of RDE is 200 ms. The time resolution of current recorder is 100 ms. It enables to follow the homogenization of concentration in reaction vessel after analyte addition. The result can be seen in fig. 10.

The result on the fig. 10 demonstrates the dependence of the RDE response on its geometry. It shows typical response of classical RDE and RDE with wider disk. In both cases the material of electrode was polished platinum wire of 2 mm diameter melted in glass. The angular velocity was the same 62 s^{-1}. The response time of both electrodes was 200 ms at sampling time 100 ms electronic recorder.

The electrode with a 3 mm diameter (Fig. 10a) has significantly lower noise (0.1 nA – inserted noise analysis). The noise was analyzed when fluctuations of the signal disappeared. These fluctuations are caused by homogenization of the concentration in the bulk of solution. The homogenous concentration is reached after 180 s (3 min.). The electrode with a 10 mm (additional disk but the active area is same as in case of previous one) stabilizes significantly faster but with greater noise (7 nA – inserted noise analysis). The fluctuation of signal differs significantly from the previous arrangement and the concentration is homogenous in 15 s. Similar influence can be seen in dependence of signal on the distance of RDE and bottom of reaction vessel (Sajdlova, 2010).

2.4.2 Measurement of glucose oxidase by electrochemical sensor with immobilized enzyme

The measurement was done by the same procedure as in case of H_2O_2 only the sensor with immobilized glucose oxidase on the AC1.W2.RS was used in microfluidic system (MFS) with wall-jet reaction chamber. In Fig. 11 there is the calibration curve. The flattening of the calibration curves at higher concentrations is dictated by Michaelis-Menten kinetics. It is possible to see that at lower levels the enzyme reaction approximates the first order kinetics whereas at highest concentrations the reaction order approaches zero and the measured current becomes independent of glucose (enzyme substrate) concentration (Mell & Maloy, 1974)

The wide measured concentration range and extremely low limit of detection is the result of nanostructure as mentioned in section 1. The immobilization is made by this manner that

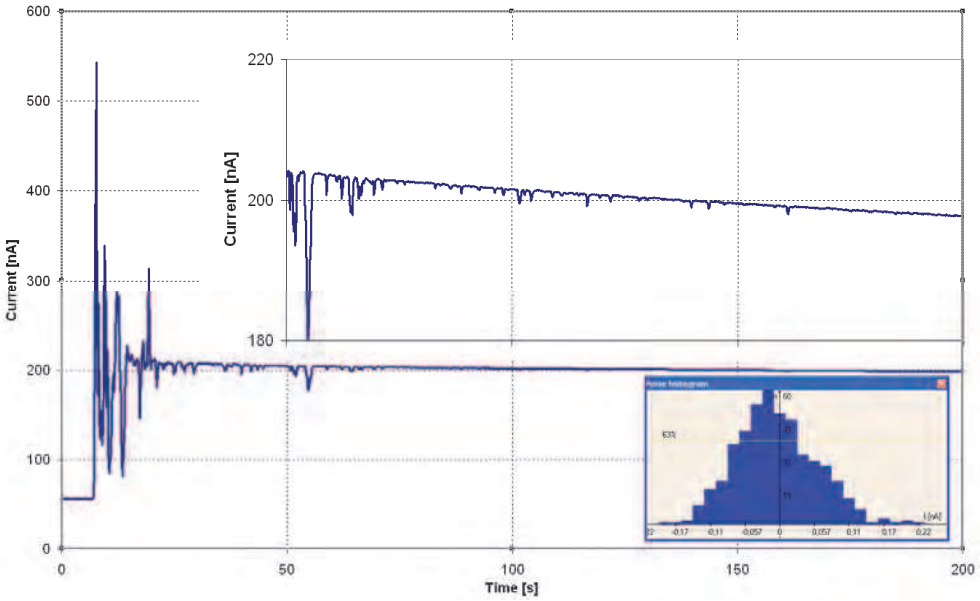

(a)

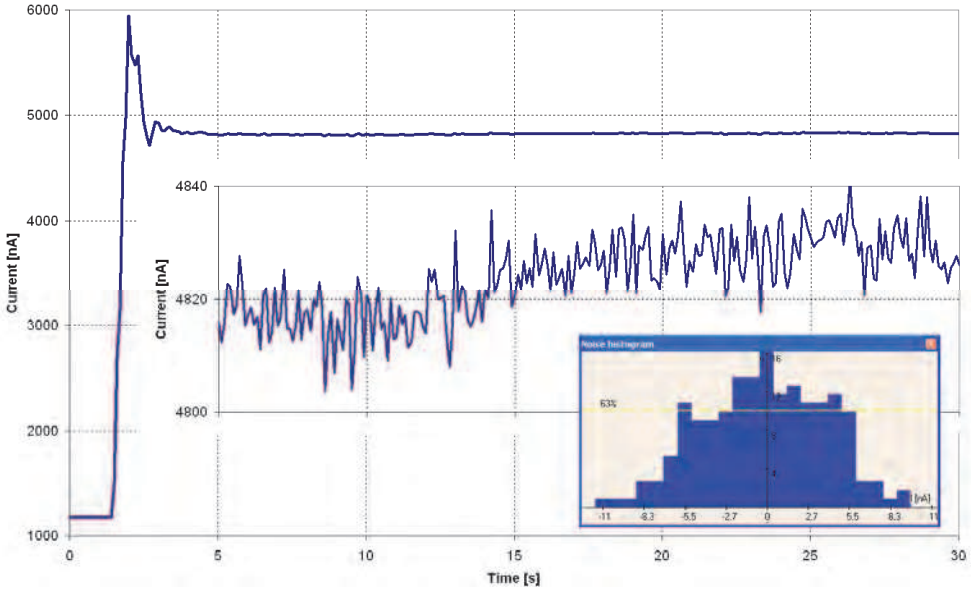

(b)

Fig. 10. The response to addition of analyte of the RDE of diameter a) 3 mm in 5 ml buffer and b) 10 mm diameter in 5 ml buffer.

the bioactive layer fills the free space between grains of Pt. It assures very tight connection between immobilized enzyme and active Pt surface. The overall active layers thickness (Pt and immobilized enzyme) is about 5 x 10^{-3} mm. This assures the respond time less than 1 s.

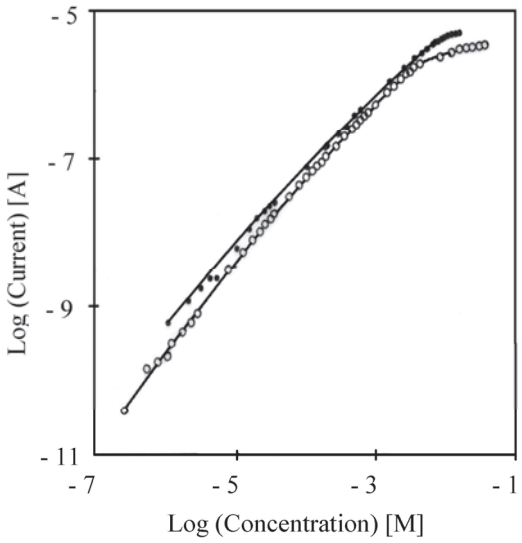

Fig. 11. Calibration curves of glucose biosensor in stirred vessel (•) and in the microflow system (○)

2.4.3 The measurement of soluble enzyme activity

The measurement of soluble enzymes activity is based on simplified Michaelis-Menten equation (Macholán, 1991). It can be written on condition [S] > 100 K_M i.e., the initial slope of the record of reaction of substrate with enzyme is proportional to the enzyme activity. The precision of approximation is better than 1 %. The absolute H_2O_2 production in mols can be recalculated for known volume of reaction vessel. It enables to calculate the activity of GOD sample addition. The same experiment was done with RDE at same conditions (ω = 60 s^{-1}), see section 2.4.1. The measurement principle has been depicted in the fig. 12a on an example of GOx. After the reaction vessel was filled with 5 ml of glucose solution of concentration 0.5 M ([S] ≈ 100 K_M) the observation was started and the background current measurements were recorded (A). The current response of the sensor was calibrated trough addition of aliquot of product, i.e., H_2O_2 (B). Then the solution of enzyme (GOx) was added (C). With the reaction initiation the current started rising linearly (D). The slope of current rising describes production of H_2O_2. The international unit of enzyme activity is defined for GOx as an amount of enzyme which oxidized 1 μmol of D-glucose to gluconolacton and H_2O_2 per 1 minute, at temperature 35 °C and at pH 5.1. The resulting calibration curve is in fig. 12b for MFS and RDE. The results of RDE are significantly better (lower limit of detection) which is caused by better time resolution of RDE and better long term stability of RDE current. Better long term stability enables higher resolution of extremely small changes of current slope.

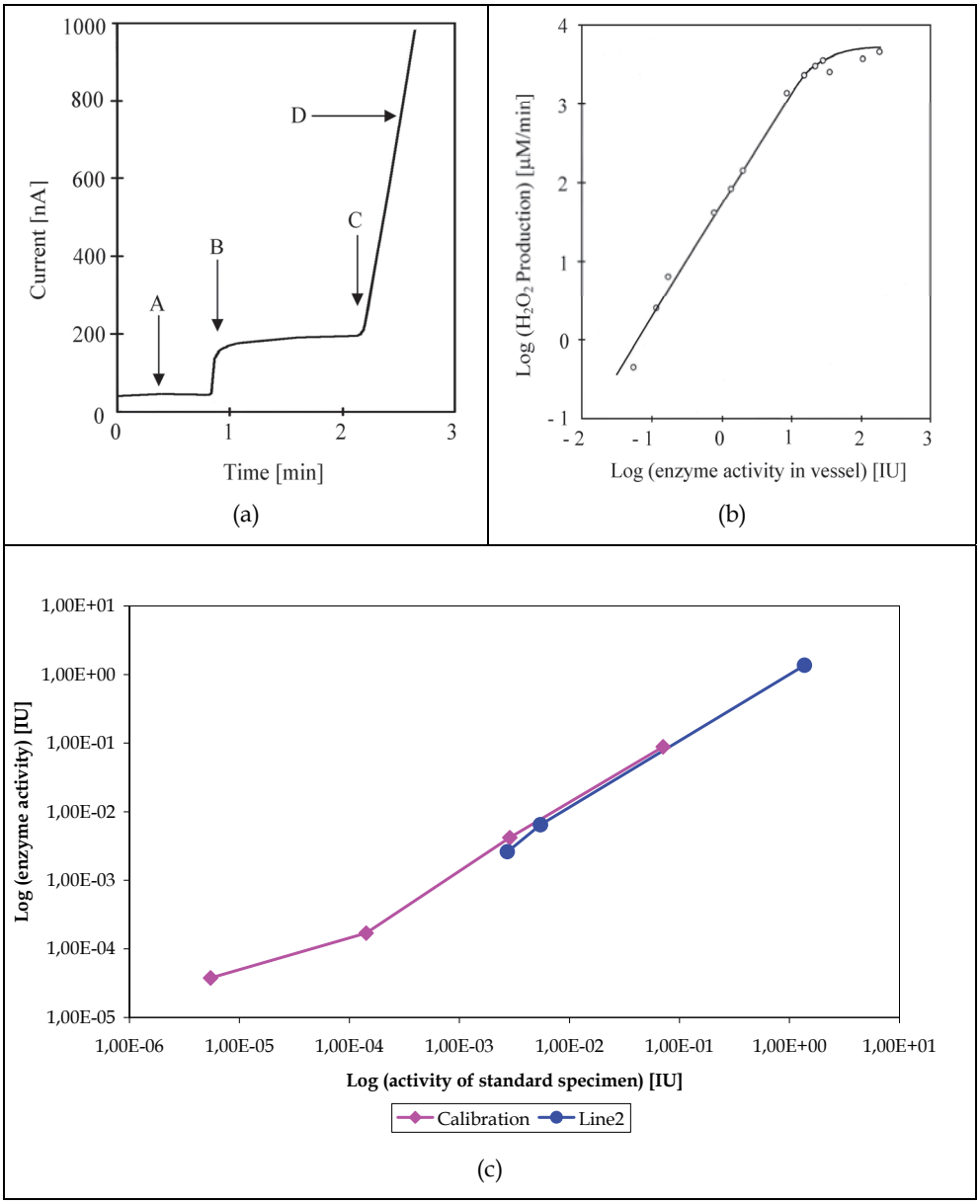

Fig. 12. a) Schematic view of enzyme activity measurement; A) addition of glucosse concentration in vessel c_{vessel} = 500 mM; B) addition of H_2O_2 for calibration c_{vessel} = 20.2 µM; C) injection of GOx solution of unknown activity; D) H_2O_2 production (478 µM/min).
b) Calibration curve for enzyme activity measurement using MFS (Krejci et al., 2008).
c) Calibration curve for enzyme activity measurement using RDE.

2.4.4 Cyclic voltammetry (CV) at temperature gradient

Measurements were performed in a device consisting of a glass cell TC1, conic stirrer and connector KSA1 and electrochemical sensor AC1.W2.RS (H, T) (BVT Technologies, Czech Republic). The AC1.W2.RS (H) electrochemical sensor bears platinum working and auxiliary electrodes, a pseudo-reference silver electrode and a heating circuit. The cell TC1 was placed in a small thermostat TK-1 (KEVA, Czech Republic). The whole system schematic is shown in figure 8 (Krejci et al., 2010).

CV is the most common electrochemical method used to investigate the electrochemical behaviour of an analyte. It enables the investigation of electrode reaction which occurs in the proximity of electrode (Bard & Faulkner, 1980; Riger, 1993; Riley & Tomlinson, 1987). On the other hand the hysteresis of cyclic voltammety curves which is related to mass transport (one compounds is cumulated at the electrode during reduction scan which is reoxidized under oxidation scan) makes the evaluation of CV quite difficult and more or less dependent on the experience of evaluator. The improvement by the string does not work because of causing noise. However the improving of mass transport by thermo diffusion significantly improves the CV and facilitates its evaluation. The improvement can be seen in fig 13.

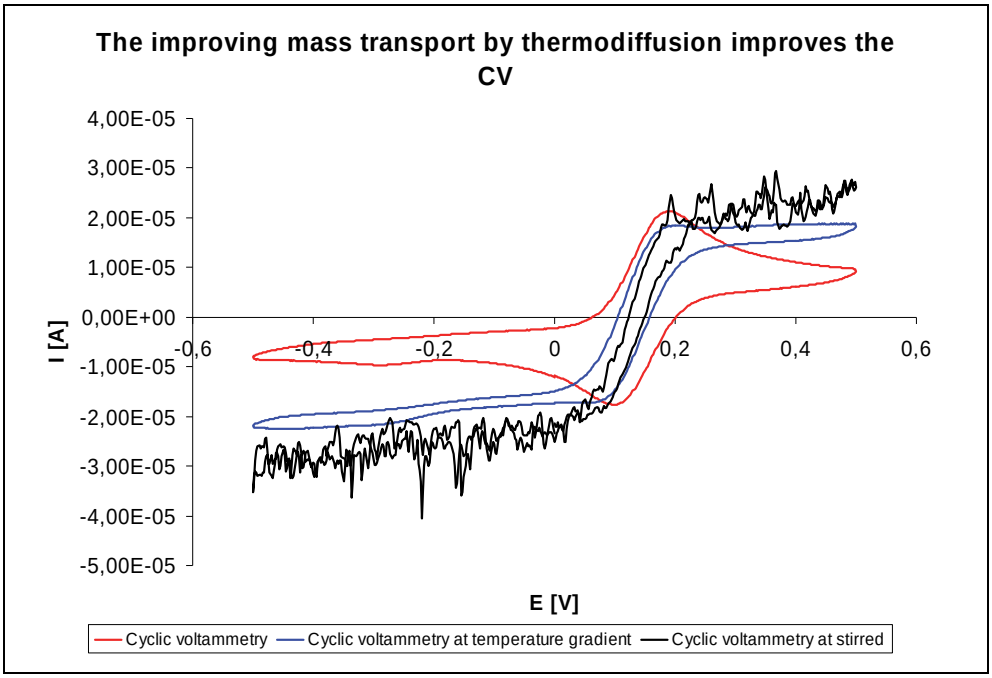

Fig. 13. The improving of mass transport by thermo diffusion

The samples of CV with thermo diffusion mass transport agree with equation (10) and it can be used to measurement of E_0 at given temperature. Due to high thermal conductivity of ceramic sensor base and precise temperature measurement using Pt 1000 thermometer integrated in the proximity of working electrode the dependence of $E_0(T)$ can be measured. The temperature difference about 10 – 40 °C significantly improves the mass transport and measured current.

3. Conclusion

The importance of mass transport has been discussed, namely with respect to screen printed electrodes. The technology of screen printing and more general application of microelectronic technologies open new area for electrochemical sensor application. However their effective use relies on a clear and comprehensive understanding of mass transport between electrode surface and bulk of solution. Advances with micro fluidics can significantly help, as demonstrated using the micro fluidic system (MFS) with wall-jet and thin layer micro fluidic arrangement. The classical arrangement of RDE can be miniaturized and produced at significantly lower cost. Consequently disposable RDE can be used as highly efficient tools for immobilized enzyme investigation, for optimization of the immobilization process and enzymatic membrane kinetic measurement as well as other parameters important for the immobilization process. Screen printing is a subset of Thick Film Technology used in microelectronics. This enables the integration not only of the sensor active electrodes but also heating elements and thermometers. Such complicated integrated sensors offer new possibility to improve mass transport form the bulk of solution to the active electrode surface. An example is thermo diffusion which may simplify the evaluation of CV. The importance of mass transport was discussed, namely with respect of screen printed electrodes. The technology of screen printing and more generally application of microelectronic technologies opens new area of electrochemical sensor application.

4. Acknowledgment

This work was supported by the EU 7th Framework Programme 230749, EU 7th Framework Programme 262007 and Czech Science Foundation KAN200520702. I would like to thank Mark O'Connell from Probe Scientific for help with English text.

5. References

Bard, A.J.; Faulkner, L.R. (1980). Electrochemical Methods-Fundamentals and Applications. John Wiley & Sons. New York. USA

Brunt K.; Bruins C.H.P. (1979). Evaluation of the characteristics of the differential amperometric detector in combination with anion-exchange chromatography, using l-ascorbic acid as test compound. Journal of Chromatografy A, Vol.172, Issue 1, pp. 37-47

Clark, L.C.; Lyons, C. (1962). Ann.N.Y. Acad.Sci., Vol.102, pp. 29-45.

Dock, E.; Christenson, A.; Sapelnikova, S.; Krejci, J.; Emnes, J.; Ruzgas, T. (2005). A steady-state and flow-through cell for screen-printed eight-electrode arrays. Analytica Chimica Acta, Vol. 531, pp. 165–172.

Dvořák, J.; Koryta, J. (1983). Elektrochemie. Academia, nakladatelství ČSAV, Praha

Frost and Sullivan. (1994). Technnical insights, A.D.Litlle in Transducer aspects of biosensors, Sethi, R.S., Biosensors and Bioelectronics 9, 243-264

Hanekamp H.B.; Nieuwkerk H.J. (1980). Anal. Chim., Acta 121, pp. 13-22.
http://www.lorentzcenter.nl/lc/web/2008/317/presentations/Baltruchat.pdf

Chan, F.-L.; Chang,W.-Y.; Kuo, L.-M.; Lin, Ch.-H.; Wang, S.-W.; Yang,Y.-S.; Lu, M. S-C. (2008). IOP publishing journal of micromechanic and microengineering. Vol.18, No.12.

Karman, T. (1921); Uber laminare and turbulente Reibung. Zeitschrift fur angewandte Mathematik und Mechanik, Vol.1, No.4, pp. 233-252.

King, P.; Prasard,V. S. R. K.; Rao, G. H. (2005). Indian Journal of Chemical Technology, pp. 455-461.
Kotyk, A.; Horák, J. (1977) Enzymová kinetika. Academia, Praha
Krejci, J. (1988). Glucose sensor – Internal report. Research institute of medical engineering, Brno
Krejci, J.; Lacina, K.; Vránová, H.; Grosmanová, Z. (2008). Microflow Vessel Improvning Reproducibility and Sensitivity of Electrochemical measurements. Electroanalysis 20, No.23, pp. 2579-2586.
Krejci, J.; Sajdlová, Z.; Krejci, J., Jr.; Marvanek, T. (2010). Voltammetry under Controlled Temperature Gradient. Sensors, Vol.10, pp. 6821-6835.
Levich, V.G. (1962) Physicochemical Hydrodynamics. Prentice Hall, Inc. Englewood Cliffs, N.J.
Levich, V.G. (1947). Discuss. Faraday Soc. 1, Vol.37.
Levich, V.G. (1944). Acta Physicochem. USSR 19, Vol.113.
Levich, V.G. (1944). Acta Physicochem. USSR 19, Vol.117.
Levich, V.G. (1942). Acta Physicochem. USSR 17, Vol.257.
Levich, V.G. (1947). Disc. Faraday Soc. 1, Vo.37.
Macholán, L. (1991) Biocatalytic Membrane Electrodes in. Bioinstrumentation and Biosensors. Wise, L. D. (ed.); Dekker, M. New York-Basel-Honkong
Maly, J.; Krejci, J.; Ilie, M.; Jakubka, L.; Masojidek, J.; Pilloton, R.; Sameh, K.; Steffan, P.; Stryhal, Z.; Sugiura, M. (2005). Analytical and Bioanalytical Chemistry, Vol.381, pp. 1558-1567.
Masavaťˇ, P.; Liawruangrath, S. (2008). Chiang Mai J. Sci., Vol.35, pp. 355-369.
Matsuda H. (1967). J. Electroanal. Chem., Vol.15, pp. 325-336.
Matsuda H. (1967). J. Electroanal. Chem., Vol.15, pp. 109.
Mell, L.D.; Maloy, J.T. (1974). Anal. Chem., Vol.47, pp. 299-307.
Painton, C.C.; Mottola, H.A. (1983). Anal. Chim. Acta 154, pp. 1-16.
Polyanin, A.D.; Kutepov, A.M.; Vyazmin, A.V.; Kazenin, D.A. (2002). Hydrodynamics, Mass and Heat Transfer in Chemical Engineering. London and New York, Taylor & Francis
Riger, P.H. (1993). Electrochemistry. Chapman & Hall, New York
Riley, T.; Tomlinson, C. (1987) Principles of Electroanalytical Methods. New York: John Wiley & Sons
Sajdlová, Z. (2010). Ph.D. thesis, Elactrochemical detector with electrodes array and rotating disk
Sethi, R. S.; Gray Stephens, L. D.; Bruce, N. C.; Lowe, C. R.. An Improved Silicon Chip Based Biosensor in "Proc.Third International Meeting on Chemical Sensors" Cleveland, Ohio, USA, 116-117, 24/26 September (1990).
Sethi, R. S. Silicon Processing in the Fabrication of Biosensors. Semiconductor International, NEC, Birmingham, UK, 14-16 March (1989).
Todd M. Squires; Robert J. Messinger & Scott R. Manalis. (2008) Nature Biotechnology
Tóth, K.; Štulík, K.; Kutner, W.; Fehér, Z.; Lindner, E. (2004). Pure Appl. Chem., Vol.76, No.6, pp. 1119-1138
Turner, A.P.F.; Karube, I.; Wilson, G. S. (1987) eds.: "Biosensors: Fundamentals and Applications", Oxford Press, Oxford
Updike, S.J.; Hicks, G. P. (1986). The Enzyme Electrode. Nature 214, pp. 986-988
Wranglén G.; Nilsson O. (1962). Electro chim., Acta 7, pp. 121-137.
Yamada J.; Matsuda H. (1973). J. Electroanal. Chem., Acta 44, pp. 189-198.

New Perspectives in Biosensors Technology and Applications

Edited by Prof. Pier Andrea Serra

ISBN 978-953-307-448-1
Hard cover, 448 pages
Publisher InTech
Published online 27, July, 2011
Published in print edition July, 2011

A biosensor is a detecting device that combines a transducer with a biologically sensitive and selective component. Biosensors can measure compounds present in the environment, chemical processes, food and human body at low cost if compared with traditional analytical techniques. This book covers a wide range of aspects and issues related to biosensor technology, bringing together researchers from 12 different countries. The book consists of 20 chapters written by 69 authors and divided in three sections: Biosensors Technology and Materials, Biosensors for Health and Biosensors for Environment and Biosecurity.

INTECH
open science | open minds

InTech Europe
University Campus STeP Ri
Slavka Krautzeka 83/A
51000 Rijeka, Croatia
Phone: +385 (51) 770 447
Fax: +385 (51) 686 166
www.intechopen.com

InTech China
Unit 405, Office Block, Hotel Equatorial Shanghai
No.65, Yan An Road (West), Shanghai, 200040, China
中国上海市延安西路65号上海国际贵都大饭店办公楼405单元
Phone: +86-21-62489820
Fax: +86-21-62489821